ARTICLES
https://doi.org/10.1038/s41564-019-0431-8
nature microbiology

The *Toxoplasma* effector TEEGR promotes parasite persistence by modulating NF-κB signalling via EZH2

Laurence Braun[1], Marie-Pierre Brenier-Pinchart[1], Pierre-Mehdi Hammoudi[1], Dominique Cannella[1], Sylvie Kieffer-Jaquinod[2], Julien Vollaire[3], Véronique Josserand[3], Bastien Touquet[4], Yohann Couté[2], Isabelle Tardieux[4], Alexandre Bougdour[1*] and Mohamed-Ali Hakimi[1*]

The protozoan parasite *Toxoplasma gondii* has co-evolved with its homeothermic hosts (humans included) strategies that drive its quasi-asymptomatic persistence in hosts, hence optimizing the chance of transmission to new hosts. Persistence, which starts with a small subset of parasites that escape host immune killing and colonize the so-called immune privileged tissues where they differentiate into a low replicating stage, is driven by the interleukin 12 (IL-12)–interferon-γ (IFN-γ) axis. Recent characterization of a family of *Toxoplasma* effectors that are delivered into the host cell, in which they rewire the host cell gene expression, has allowed the identification of regulators of the IL-12–IFN-γ axis, including repressors. We now report on the dense granule-resident effector, called TEEGR (*Toxoplasma* E2F4-associated EZH2-inducing gene regulator) that counteracts the nuclear factor-κB (NF-κB) signalling pathway. Once exported into the host cell, TEEGR ends up in the nucleus where it not only complexes with the E2F3 and E2F4 host transcription factors to induce gene expression, but also promotes shaping of a non-permissive chromatin through its capacity to switch on EZH2. Remarkably, EZH2 fosters the epigenetic silencing of a subset of NF-κB-regulated cytokines, thereby strongly contributing to the host immune equilibrium that influences the host immune response and promotes parasite persistence in mice.

Caused by the protozoan Apicomplexa *Toxoplasma gondii*, toxoplasmosis is one of the most widespread foodborne parasitic zoonosis on earth and poses a significant risk to public health, mostly in cases of immune dysfunction. Triggered by the initial colonization of intestinal mucosa by *T. gondii*, the interleukin 12 (IL-12)–interferon-γ (IFN-γ) axis plays a prominent role in anti-parasite immunity as it halts the acute expansion of the *T. gondii* 'tachyzoite' population in host cells and throughout the host, yet it also promotes the establishment of the long-term persistent 'bradyzoite' stages in cells of deep tissues[1]. At the heart of this immune context lies the remarkable ability of tachyzoites to actively reshape gene expression of the host cell owing to a large number of effector molecules pre-stored in secretory organelles[2]. First, effectors contained in the apical rhoptry organelles (ROP proteins) are injected directly into the host cell cytoplasm at the very onset of cell invasion before the tachyzoite gets enclosed in a parasitophorous vacuole. Following parasitophorous vacuole formation, effectors from the dense granules, namely the GRA proteins, are exocytosed by the tachyzoite in the lumen of the parasitophorous vacuole; they further either reside at the host–parasite interface or are exported in the host cell[3]. Therefore, some GRA proteins are featured to cross the parasitophorous vacuole membrane and a subset of these can even traffic to the host cell nucleus where they gather into hyper-stable complexes of proteins that usually do not assemble in uninfected cells. Founder members include GRA16[4], GRA24[5] and TgIST[6,7], all of which contribute to the building of functional networks in infected cells by interfacing with the host signalling pathways or co-opting host transcription factors[8].

Here, we identified *Toxoplasma* E2F4-associated EZH2-inducing gene regulator (TEEGR) as a dense granule-resident effector and demonstrated its unique regulatory function on the activity of E2F–DP transcription factors and consequently on the expression of the epigenetic silencer EZH2 in the host cell. These functional features provide TEEGR with a pivotal role in mediating a regulatory control loop that antagonizes the nuclear factor-κB (NF-κB)-driven pro-inflammatory responses to *T. gondii* infection.

Results

TEEGR is a dense granule-resident protein exported to the host cell nucleus. TEEGR was originally identified in a repertoire of intrinsically disordered *T. gondii* proteins (Fig. 1a) that are singularly exported into the nucleus of the infected cell[4]. The protein exhibited a characteristic punctate distribution pattern in the parasite cytoplasm and occasionally overlapped with the dense granule GRA7 but remained excluded from the apical rhoptry and microneme organelles, as verified with the canonical toxofilin and MIC2 markers, respectively (Fig. 1b and Supplementary Fig. 1). Once the parasites were enclosed in the parasitophorous vacuole, TEEGR was detected in the parasitophorous vacuole space and beyond the parasitophorous vacuole membrane in the host cell nuclei while the parasitophorous vacuoles continued to enlarge along with parasite multiplication. Its localization in the host cell nucleus was seen as early as 6 h post invasion (Fig. 1c). In agreement with a shared export

[1]Team Host-Pathogen Interactions and Immunity to Infection, Institute for Advanced Biosciences, INSERM U1209, CNRS UMR5309, Université Grenoble Alpes, Grenoble, France. [2]Université Grenoble Alpes, CEA, INSERM, Grenoble, France. [3]OPTIMAL Small Animal Imaging Facility, Institute for Advanced Biosciences, Grenoble, France. [4]Team Membrane and Cell Dynamics of Host Parasite Interactions, Institute for Advanced Biosciences, INSERM U1209, CNRS UMR5309, Université Grenoble Alpes, Grenoble, France. *e-mail: alexandre.bougdour@inserm.fr; mohamed-ali.hakimi@inserm.fr

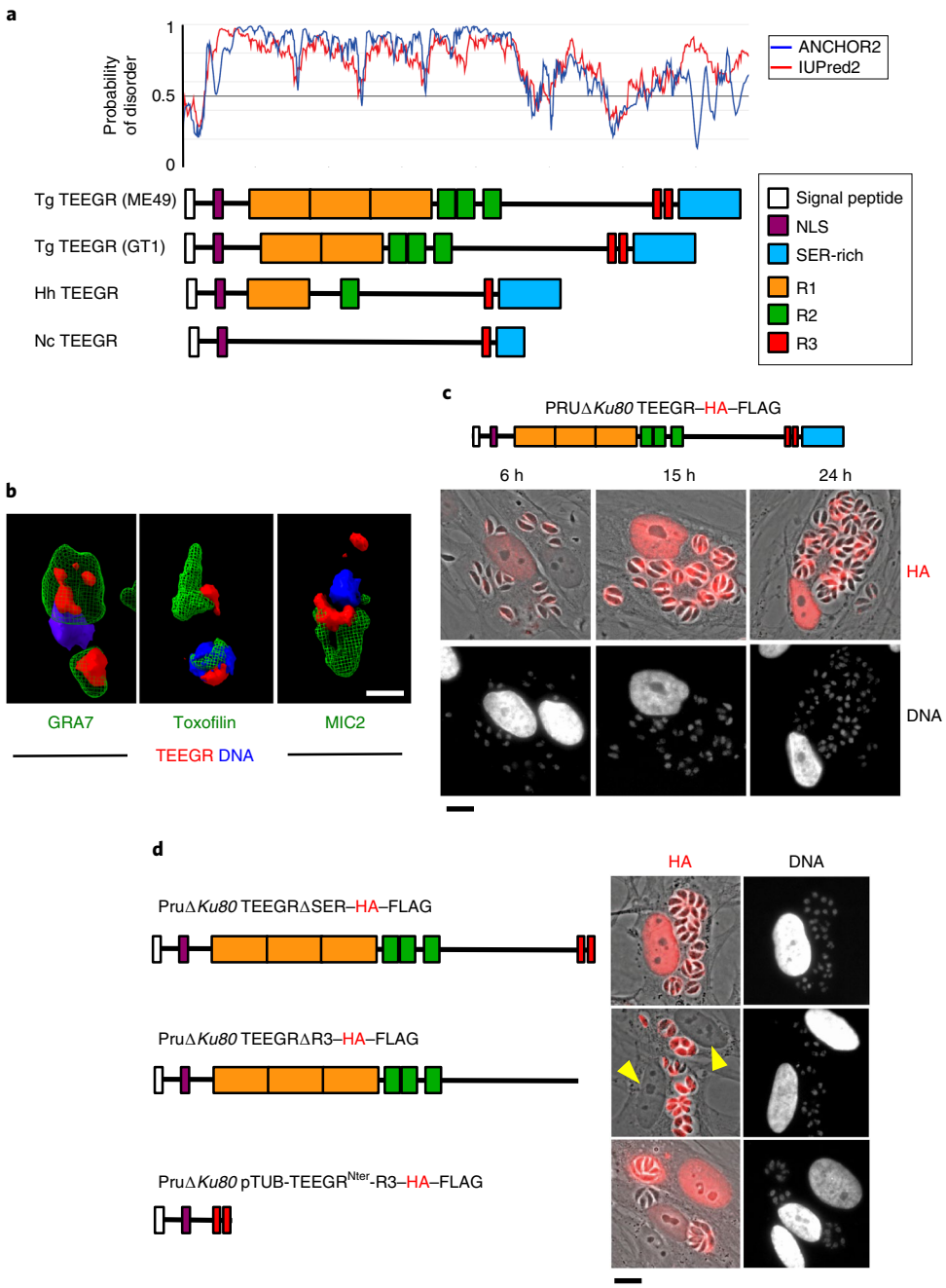

Fig. 1 | The export of TEEGR in the host cell nucleus. The gene *TGME49_239010* encoding TEEGR was originally identified in silico together with GRA16[4], GRA24[5] and TgIST[6,7] as strong parasite candidate genes with attributes to both target the parasite secretory pathway and reach the host cell nuclei. **a**, TEEGR is a highly disordered 80 kDa protein (predicted disorder score >0.5) that carries a signal peptide, a putative nuclear localization sequence (NLS) and multiple repeated domains (R1, R2 and R3) whose repeat number and distribution have evolved through coccidian subclasses and among *T. gondii* lineages. Tg, *Tgondii*; Nc, *N. caninum*; Hh, *Hammondia hammondia*. **b**, HA–FLAG-tagged TEEGR in PruΔ*ku80* extracellular parasites is contained in cytoplasmic organelles distinct from the apical micronemes (MIC2) and rhoptries (Toxofilin) and partially co-localizes with the dense granule protein GRA7. Cells were co-stained with Hoechst DNA-specific dye. Scale bar, 1 µm. **c**, Time course of TEEGR secretion and export to the host cell nucleus. HFFs were infected with PruΔ*ku80* TEEGR–HA–FLAG parasites (top) and stained with anti-HA antibodies (bottom). Scale bar, 10 µm. **d**, In situ subcellular localization of TEEGR chimeric proteins (red; right) in HFFs infected with parasites expressing endogenously HA–FLAG-tagged TEEGR truncated proteins (TEEGRΔSER and TEEGRΔR3) or TEEGR^{Nter}-R3 expressed under the control of a TUB8 promoter (left). Yellow triangles indicate the nuclei of infected cells negative for TEEGR export. Scale bar, 10 µm. All data are representative of three independent biological experiments.

mechanism between GRA proteins[8], the translocation of TEEGR across the parasitophorous vacuole membrane was dependent on the translocon protein MYR1 and, even on the aspartyl protease ASP5, in spite of any detectable TEXEL motif (Supplementary Fig. 2). Peculiarly, TEEGR export was prevented by the deletion of the repeat 3 (R3)-containing C-terminal domain (TEEGRΔR3), which presumably impacted the step of secretion into the parasitophorous vacuole space (Fig. 1d). In the same line, the addition of R3 repeats to the extreme N-terminus region of TEEGR was sufficient to drive the chimeric protein to the host cell nucleus, its final destination

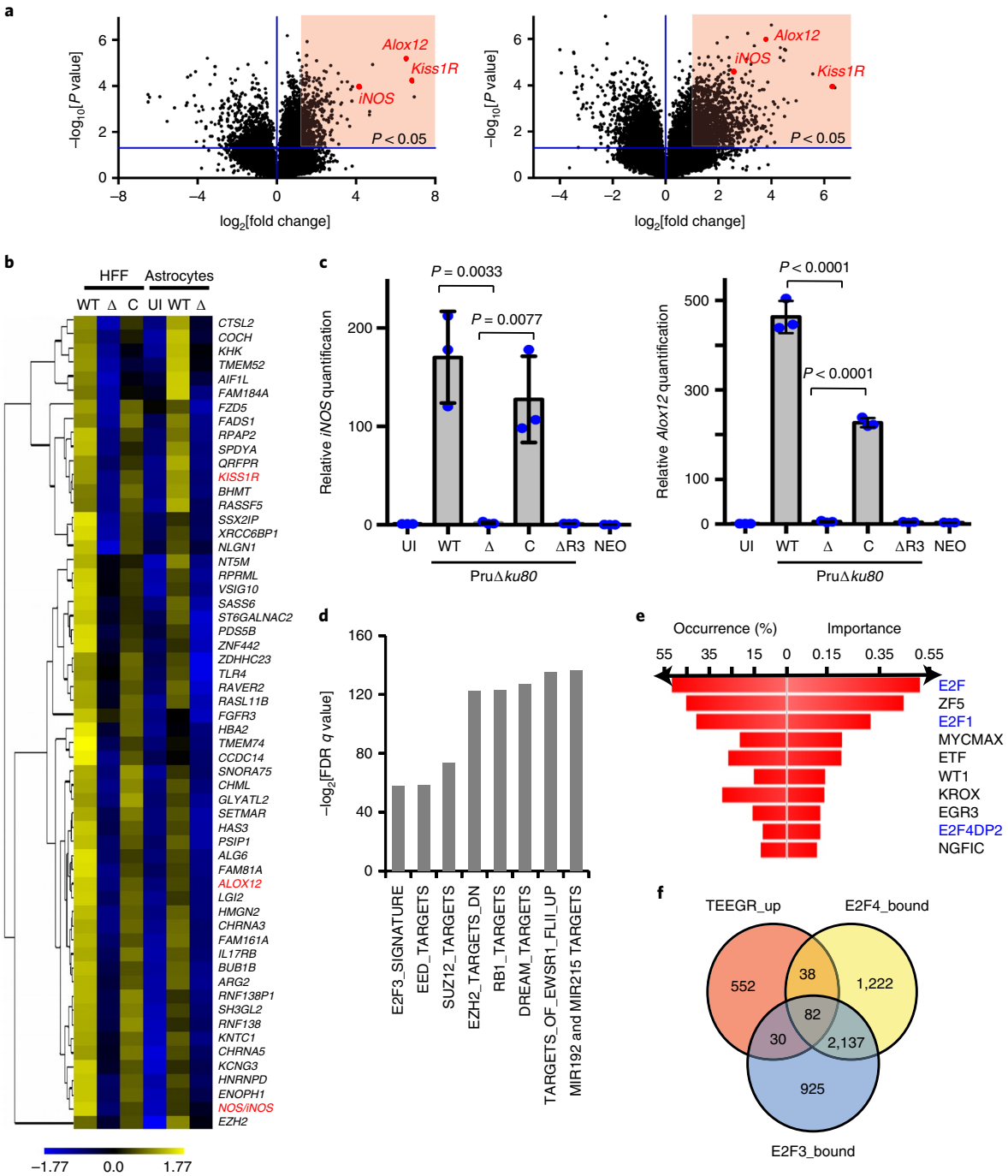

Fig. 2 | TEEGR activates gene expression in human cells in a E2F3 and E2F4-dependent manner. Genome-wide expression profiling of human fibroblasts and astrocytes infected with the Δ*teegr* mutant (Δ), parental type II strain PruΔ*ku80* (WT) and trans-complemented strain (C). **a**, The results of tests for differential expression between the Δ*teegr* mutant and the parental strain in HFFs (left) and astrocytes (right) are presented as volcano plots that plot the statistical significance against fold change for each gene. The genes (HFFs, $n = 784$ and astrocytes, $n = 1{,}529$; in red squares) with adjusted $P \leq 0.05$ (Bonferroni-corrected) and absolute fold changes of ≥1.5 are deemed of interest for in silico pathway analyses (Supplementary Table 1). **b**, Heat map of the expression values for differentially expressed genes in human cells infected with WT, Δ and C parasites. The mean $\log_2$ gene expression values were median centred for the 472 genes (more than fourfold; $P < 0.05$, unpaired *t*-test) that were defined as core TEEGR-regulated genes in HFFs and human astrocytes; the genes were clustered by hierarchical clustering based on a Pearson's correlation and a heat map with 58 genes is presented. The complete set of genes is listed in Supplementary Table 1. **c**, HFF cells were either uninfected (UI) or infected for 24 h with WT, Δ, C or TEEGRΔR3 (ΔR3) parasites. The levels of *iNOS* (left) and *Alox12* (right) mRNA were determined by RT–qPCR. The values were normalized to the amount of *β2-microglobulin*. Data are the mean ± s.d. of three biological replicates. *P* values were calculated using a two-tailed unpaired Student's *t*-test. NEO, *Neospora caninum*. **d**, GSEA of the 784 genes positively regulated by TEEGR in HFF cells (Supplementary Table 1) highlighted eight gene expression signatures of chemical and genetic perturbations that were significantly and selectively enriched ($P < 0.05$, FDR-corrected; two-sided Welch *t*-test). **e**, TFBS analysis of the 784 TEEGR-upregulated genes was performed by DiRE analysis and the ten most significant transcription factors are listed. Transcription factors belonging to the E2F family are indicated in blue. **f**, Venn diagram illustrating the overlap between the number of genes upregulated by TEEGR (more than twofold; $P < 0.05$, unpaired *t*-test) in HFFs and the number of genes identified as E2F3- or E2F4-bound by Julian et al.[11] and Marson et al.[10], respectively.

(Fig. 1d). Regardless of its atypical mechanism of delivery, TEEGR is a genuine member of the subfamily of dense granule-resident proteins that are singularly exported into the host cell nuclei[8].

TEEGR activates expression of E2F3/4-regulated host genes. The detection of TEEGR in the host cell nucleus prompted us to investigate whether the protein could contribute to the re-orchestration of gene expression carried out by type II *T. gondii* genotypes in both non-haematopoietic and haematopoietic lineages. When comparing the Δ*teegr* mutant with the parental strain, we found that the expression of 784 and 1,529 human genes was indeed upregulated in a TEEGR-dependent fashion in human fibroblasts and astrocytes, respectively (Fig. 2a and Supplementary Table 1). Of these, 215 were common to both cell types and hierarchical clustering of the 58 top-ranked genes (more than fourfold, false discovery rate (FDR) <1%) delineated specific clusters of TEEGR-induced transcripts following infection (Fig. 2b). Consistent with this, reintroduction of the TEEGR gene in the Δ*teegr* strain mutant restored the expression pattern to levels observed with wild-type (WT) parasites, thereby demonstrating the TEEGR-dependent induction of those genes (Fig. 2b). Furthermore, these results were unequivocally validated with the significant increase in the messenger RNA levels of three specifically TEEGR-activated genes (*iNOS*, *Alox12* and *Kiss1R*), which was independent of the parasite strain (type I/II) and host cell type analysed. The reintroduction of a copy of the gene in *teegr*-deficient parasites was sufficient to restore expression of these genes (Fig. 2c and Supplementary Fig. 3). Although the extent to which gene expression was induced varied with the initial *T. gondii* multiplicity of infection (m.o.i.) and the time course of infection (Supplementary Fig. 3b), it is noteworthy that none of the TEEGR-induced gene products were detected in human cells infected with *Neospora caninum*, one of the closest *T. gondii* relatives (Fig. 2c), which however harbours a poorly conserved *TEEGR*-homologous gene (Fig. 1a). Finally, the strict requirement of TEEGR as a transcriptional regulator of specific target genes was further evidenced by the absence of *iNOS* and *Alox12* gene induction in cells infected by the strains in which TEEGR export was impaired, PruΔ*ku80*ΔR3, Δ*myr1* or Δ*asp5* (Fig. 2c and Supplementary Fig. 2c).

Applying gene set enrichment analysis (GSEA) allowed the identification of eight gene-expression signatures of chemical and genetic perturbations among the 784 genes positively regulated by TEEGR in infected human foreskin fibroblasts (HFFs; Fig. 2d), whereas the distant regulatory elements (DiRE) analysis pointed to enrichment in specific transcription factor binding sites (TFBS), especially for the E2F3 and E2F4 transcription factors (Fig. 2e). For instance, 87 genes were identified as bound by the dimerization partner (DP), retinoblastoma-like, E2F4 and MuvB (DREAM) complex, a complex gathering retinoblastoma-like proteins and the E2F4–DP transcription factor[9]. TEEGR showed similar activity in non-human cells with: (1) 1,129 genes upregulated in a TEEGR-dependent manner (Supplementary Fig. 4a and Supplementary Table 2) and (2) comparable chemical and genetic perturbation signatures and TFBS enrichments, which were detected by GSEA and DiRE analysis, respectively, in *T. gondii* infected murine bone marrow-derived macrophages (BMDMs; Supplementary Fig. 4b,c). Given the putative prominent role of E2F3 and E2F4 in TEEGR-mediated gene activation in both human fibroblasts and murine macrophages, we next checked whether TEEGR and E2F3/4 regulate a shared set of genes by intersecting our transcriptomic data with chromatin immunoprecipitation-sequencing (ChIP-seq) datasets that had previously allowed genome-wide definition of the position of E2F3 and E2F4[10,11]. We found that about 20 and 37% of the TEEGR-induced genes in HFFs and BMDMs, respectively (Fig. 2f and Supplementary Fig. 4d), had been previously identified as exclusive or overlapping E2F3- and E2F4-bound genes by ChIP-seq[10,11], therefore emphasising the involvement of these two transcription factors in the TEEGR pathway.

TEEGR forms distinct complexes gathering E2F–DP transcription factors. Mapping of transcriptomic changes triggered by intracellular tachyzoites in conjunction with analysis of transcription factor occupancy provided strong evidence for cooperation between TEEGR and E2F–DP at the vicinity of shared genes, yet TEEGR has no detectable DNA-binding domain. However, TEEGR in fusion with the Gal4 DNA-binding domain strongly activated the *His3* reporter gene in yeast, which favoured growth under selective conditions (up to 200 mM of 3-AT), therefore documenting the intrinsic transcriptional transactivation properties of TEEGR. This is why we hypothesized that TEEGR-mediated gene induction may be achieved by co-opting a host transcription factor similarly to the *T. gondii* TgIST GRA effector[6].

Although TEEGR is predicted to be intrinsically unstructured (Fig. 1a), it does not carry any recognizable protein short linear motifs that could suggest dedicated interacting partner(s) in the host cell nucleus where it accumulated post infection. To search for putative TEEGR partners, we performed a systematic mapping of the TEEGR interactome when ectopically expressed in uninfected yet *T. gondii*-permissive cells or in the context of cell infection. In 293-T-REx epithelial cells, TEEGR was found in a high molecular-weight complex (~500 kDa; fractions 20–26) that resisted stringent salt conditions (Fig. 3a,b and Supplementary Fig. 5a). Mass-spectrometry-based proteomic and western blot analyses allowed confirmation of the partnership between TEEGR and the E2F3 and E2F4 transcription factors in association with their DPs, DP-1 and DP-2 (Fig. 3c and Supplementary Fig. 5b)[12]. Although ectopic expression of TEEGR in 293-T-REx cells proved informative, it did not allow capturing of either the dynamic state of the TEEGR interactome over the tachyzoite intracellular growth period (that is, involving co-exported effectors) or the complexity brought by the specific combination of given strains and host cell types. Importantly, the TEEGR–E2F–DP-containing complexes were purified from murine J774 macrophages when infected with tachyzoites from either type I or II strains that expressed epitope-tagged TEEGR (Fig. 3d and Supplementary Fig. 5c). Together, these data uncovered a multivalent partnership of TEEGR with the host E2F–DP transcription factors and validated the relevance of these interactions in the context of not only human non-haematopoietic but also murine haematopoietic lineages, regardless of the *T. gondii* infecting strain.

TEEGR induces the E2F3/4-dependent expression of the PRC2 subunit Ezh2. Apart from the TEEGR-induced genes, the expression of which has been associated with E2F3 and E2F4 transcription-factor activities, a significantly wider set of upregulated genes is likely to be controlled by other transcription factors (Fig. 2f and Supplementary Fig. 4d). Transcriptomic analysis identified miscellaneous transcription factors and chromatin-modifying enzymes among which the Polycomb group gene *EZH2* whose expression was TEEGR-induced in both murine and human cells, regardless of the parasite strain (Fig. 4a,b). EZH2 is the catalytic subunit of the polycomb repressive complex 2 (PRC2) that drives the addition of methyl groups to histone H3 at lysine 27 (H3K27me3), and ultimately mediates epigenetic transcriptional silencing during embryonic development, tumorigenesis and differentiation of immune cells[13]. Consistent with transcript profiling, EZH2 protein was never detected in primary and fully differentiated fibroblasts but clearly rose up and accumulated in nuclei of these cells once infected by *T. gondii* tachyzoites that expressed a functional version of TEEGR (Fig. 4c,d and Supplementary Fig. 5d).

As the modus operandi by which TEEGR achieves host gene activation probably depends on the E2F3 or E2F4 DNA targeting,

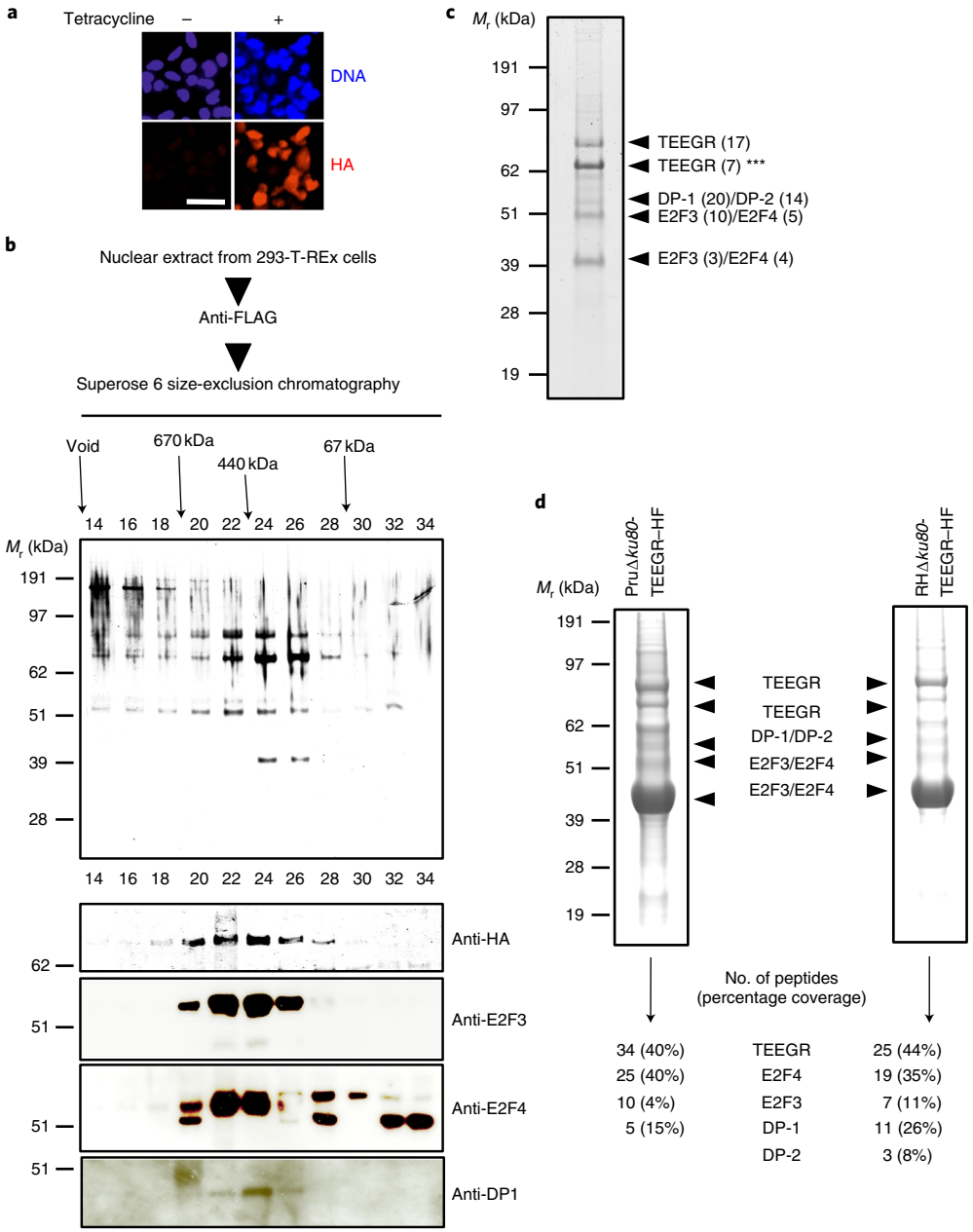

Fig. 3 | TEEGR forms a partnership with the E2F–DP host transcription factors. a, Immunofluorescence assay (IFA) of TEEGR–HA–FLAG ectopically and stably expressed in the 293-T-REx cell line. Cells were either left untreated (–) or treated (+) with tetracycline for 20 h and processed for IFA using anti-HA antibodies and Hoechst DNA-specific dye. Scale bar, 2.5 µm. **b**, TEEGR-associated polypeptides were purified from nuclear extracts of 293-T-REx cells that had been tetracycline-induced to express TEEGR–HA–FLAG. Size-exclusion chromatography of TEEGR-containing complexes after FLAG-affinity selection. The fractions were analysed on silver-stained SDS–PAGE gels (top) and blots processed to detect TEEGR–HA–FLAG (anti-HA), E2F3, E2F4 and DP-1 (bottom). **c**, Mass spectrometry-based proteomic analysis of size-exclusion chromatography fraction 24 identified the transcription factors E2F3 and E2F4 associated with DP-1/DP-2 as the only relevant TEEGR partners. The identities of the proteins with their respective number of peptides in parentheses are indicated on the right. The asterisks indicate degradation products. **d**, TEEGR-associated proteins were purified by FLAG chromatography from protein extracts of the murine J774 macrophage line infected by Pru*Δku80* TEEGR–HA–FLAG or RH*Δku80* TEEGR–HA–FLAG. Fractions were analysed on gels by silver staining and then by mass spectrometry-base proteomics to detect TEEGR and the aforementioned partners. The identity of the proteins with their respective number of peptides and percentage of coverage are indicated. All data are representative of two independent biological experiments.

we then investigated whether *EZH2* gene expression may be regulated in a TEEGR/E2F-dependent manner. In line with previous reports specifying that E2F3 and E2F4 can control *EZH2* (refs. [9,11,14]), we found that both transcription factors were enriched at the *EZH2* promoter in a TEEGR-dependent manner using ChIP-scanning analysis (Fig. 4e). Overall, TEEGR in partnership with E2F–DP positively regulates EZH2 expression, which in turn may repress host gene expression post *T. gondii* infection.

The EZH2 switch controlled by TEEGR counteracts NF-κB-dependent gene induction. Although transcriptomics unambiguously identified TEEGR as a transcriptional activator in

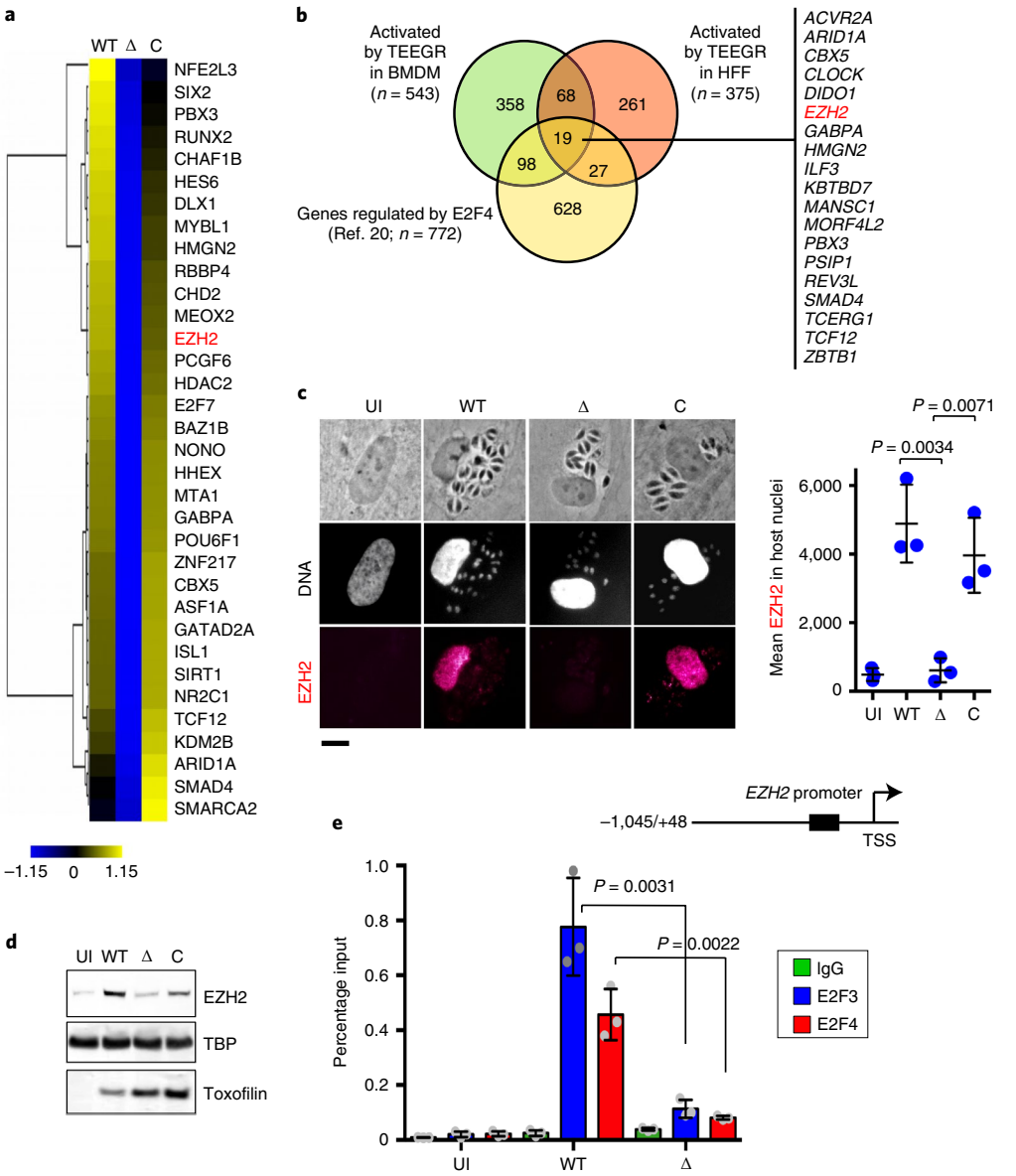

Fig. 4 | E2F3 and E2F4 DNA association with the *EZH2* promoter is enhanced by *T. gondii* infection in a TEEGR-dependent manner. a, Heat map representation of host transcription factors and chromatin-modifying enzymes upregulated in a TEEGR-dependent fashion in HFF cells infected for 24 h with the WT, Δ and C strains. EZH2 is indicated in red. **b**, Venn diagram illustrating the overlap between the number of genes upregulated by TEEGR in HFF as well as BMDM (more than twofold; $P < 0.05$, unpaired *t*-test) cells and the number of genes identified as E2F4-bound by Lee and colleagues[36]. **c**, IFA of TEEGR-dependent induction of EZH2 in HFFs that were either uninfected (UI) or infected with the WT, Δ and C strains for 24 h (left). In situ quantification of nuclear EZH2 using IFA (right). The horizontal bars represent the mean ± s.d. of the nuclear EZH2 intensity from three independent experiments ($n = 100$ nuclei per dot). Scale bar, 10 μm. **d**, Nuclear extracts from HFF cells that were uninfected or infected (24 h) with the indicated strains were analysed by western blotting using the indicated antibodies. Host-specific TBP and parasite-specific toxofilin are shown as loading controls. Data are representative of three experiments. **e**, Schematic presentation of the genomic regions corresponding to the promoter of *EZH2* (top). The black box in the *EZH2* promoter represents a region of four putative E2F sites. HFFs were either uninfected or infected for 24 h with the WT or Δ strains. Samples were analysed by a ChIP assay with specific antibodies to E2F3 and E2F4 (bottom). IgGs were used as negative controls. Bound DNA corresponding to the EZH2 promoter was quantified by quantitative PCR (qPCR)–ChIP and signals were normalized with the input DNA. Data are the mean ± s.d. of three biological replicates. *P* values were calculated using two-tailed unpaired Student's *t*-test.

infected cells (Fig. 2 and Supplementary Fig 4), it also pointed out that TEEGR triggered the repression of a sizeable fraction of host genes ($n = 494$ and $n = 571$ for human fibroblasts and astrocytes, respectively, with a twofold change and $P < 0.05$; Supplementary Table 1 and Fig. 5a). Hierarchical clustering of the 69 top-ranked genes (FDR <1%) delineated clusters of TEEGR-downregulated transcripts that were moderately induced by WT parasites but culminated with *teegr*-deficient tachyzoites (Fig. 5b). Quantitative PCR with reverse transcription (RT–qPCR) of mRNA from six of the repressed genes (that is, *IL-1β*, *IL-6*, *IL-8*, *IL-23A*, *Ptgs2* and *CCL20*) documented a robust and sustained pattern of TEEGR-mediated cytokine repression, which required TEEGR nuclear localization along with intracellular tachyzoite development (Fig. 5c

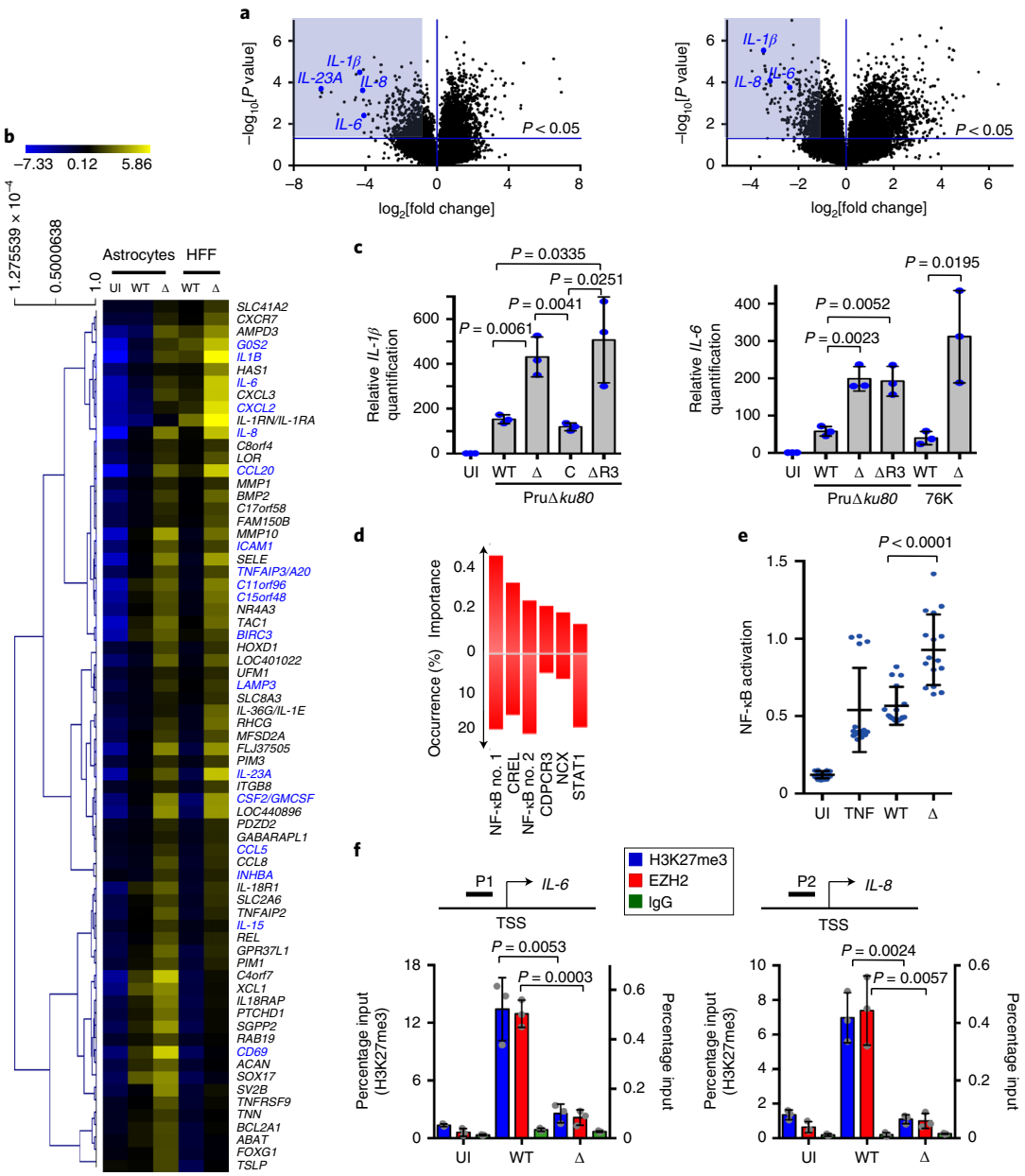

Fig. 5 | TEEGR-dependent repression of NF-κB-regulated genes is mediated by EZH2. a, Genome-wide expression profiling of HFFs (left) and human astrocytes (right) infected with WT and Δ tachyzoites. The results of tests for differential expression between WT and Δ tachyzoites are presented in a volcano plot that plots the statistical significance against the fold change for each gene. Genes coloured in blue (HFF, $n = 494$; human astrocytes, $n = 571$) have a Bonferroni-corrected $P \leq 0.05$ and absolute fold changes of ≤2 and are deemed of interest for in-silico pathway analyses (Supplementary Table 1). **b**, Heat map of the expression values of differentially expressed genes in human cells infected with WT and Δ parasites. For the 69 (more than threefold; $P < 0.05$, unpaired *t*-test) that are defined as core TEEGR-repressed genes in HFFs and human astrocytes, the mean $\log_2$ gene expression values were median centred, genes were clustered by hierarchical clustering based on a Pearson's correlation and a heat map is presented. Genes silenced by EZH2 are indicated in blue. **c**, HFF cells were either uninfected or infected for 24 h with WT, Δ, C or ΔR3 strains. The mRNA levels of *IL-1β* and *IL-6* were determined by RT–qPCR. Values were normalized to the amount of *β2*-microglobulin. Data are the mean ± s.d. of three biological replicates. **d**, TFBS analysis of the 69 TEEGR-repressed genes was performed by DiRE analysis and the top six transcription factors are listed. **e**, THP1 murine cells were treated with TNFα or infected with the PruΔ*ku80* WT or Δ*teegr* strains and then NF-κB activity was determined using a reporter gene assay (measured at OD_{630}). Data are the mean ± s.d. of 20 biological replicates. **f**, HFFs were either uninfected or infected for 24 h with WT or Δ strains. Samples were analysed by a ChIP assay with specific antibodies to EZH2 and H3K27me3. IgG was used as the negative control. Bound DNA corresponding to the *IL-6* and *IL-8* promoters (P1 and P2, respectively; top) was quantified by qPCR–ChIP and the signals were normalized to the input DNA (bottom). TSS, transcription start site. Data are the mean ± s.d. of three biological replicates. *P* values were calculated using a two-tailed unpaired Student's *t*-test.

and Supplementary Fig. 6). Accordingly, the PruΔ*ku80*ΔR3 mutant strain, for which TEEGR was retained inside the parasite (Fig. 1d), failed to induce gene repression, whereas reintroduction of the *teegr* gene in the mutant restored mRNA synthesis to basal levels and consequently the repressive gene activity driven by WT TEEGR (Fig. 5c and Supplementary Fig. 6).

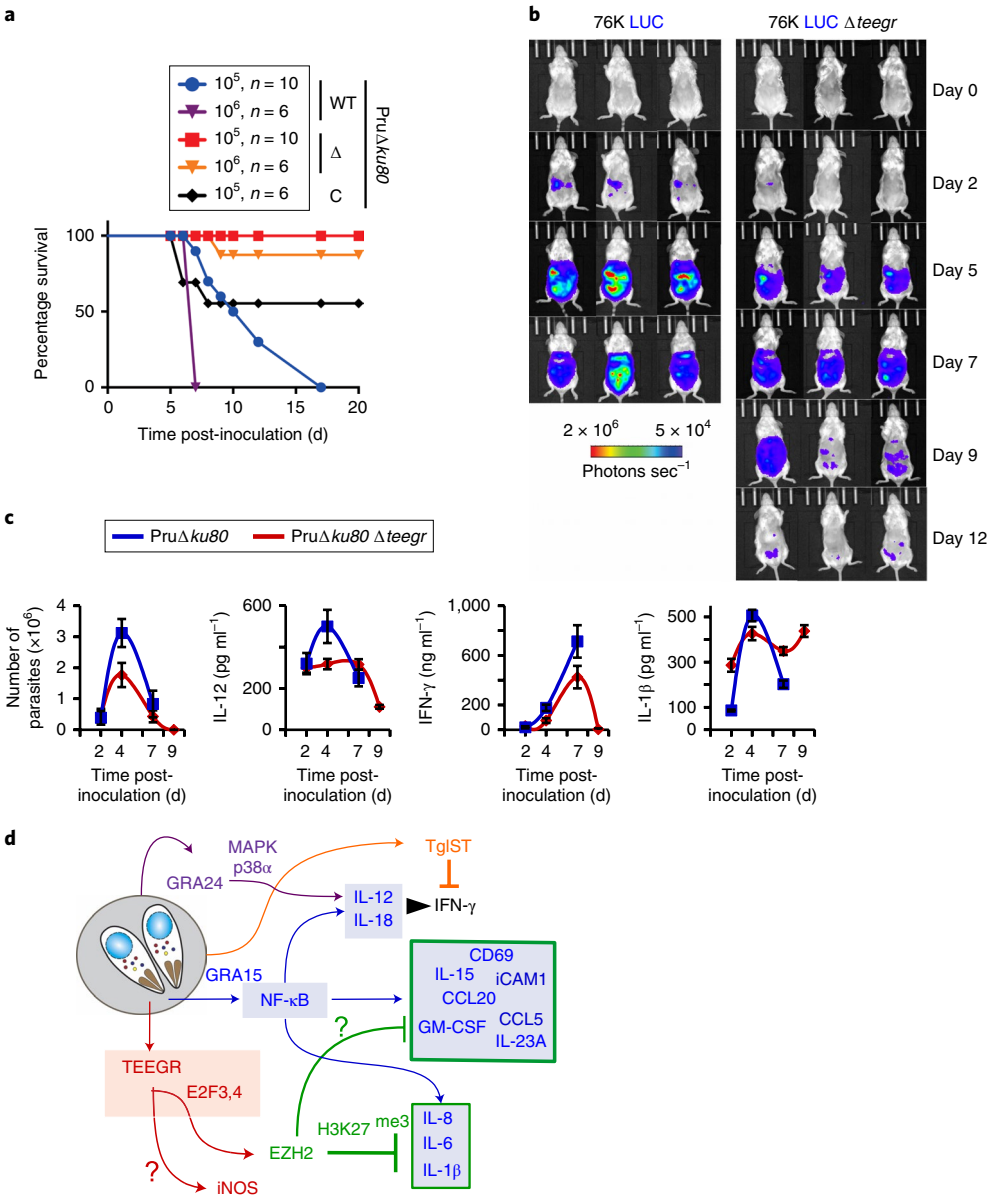

Fig. 6 | In vivo control of *teegr*-deficient *T. gondii* tachyzoite population is likely to be mediated by NF-κB-regulated pro-inflammatory cytokines. a, Mice were given either 10^5 or 10^6 tachyzoites of the WT, Δ and C strains intraperitoneally and their survival was monitored. At day 5 post-inoculation, all of the mice displayed clinical signs (weight loss and ruffled fur). Significance was tested using log-rank (Mantel–Cox; $P = 0.0161$) and Gehan–Breslow–Wilcoxon ($P = 0.0154$) tests. A two-sided $P < 0.05$ was considered statistically significant. **b**, Luminescent parasites were imaged with an IVIS imaging system from day 0–12 after the intraperitoneal inoculation of BALB/c with 5×10^4 tachyzoites per condition. The data are representative of two experiments (three mice per group). **c**, BALB/c mice were given a dose of 10^5 PruΔ*ku80* or PruΔ*ku80* Δ*teegr* tachyzoites intraperitoneally. Peritoneal lavage fluids were collected on days 2, 5, 7 and 9 post-inoculation. The number of tachyzoites in the collected samples was estimated by parasite DNA PCR and the concentrations of IL-1β, IL-12 and IFN-γ were determined by enzyme-linked immunosorbent assays (ELISAs). Data are the mean ± s.d. with $n = 3$ individual mice per parasite genotype at each time point. **d**, Schematic representation of the consequences of TEEGR delivery to the host cell by *T. gondii* tachyzoites.

The majority of the pathways significantly and selectively repressed by TEEGR clustered with biological processes that are related to immunity, particularly inflammation, as emphasised by the pole position of the NF-κB-dependent TNF-α signalling pathway (Supplementary Fig. 7a–c). The NF-κB transcription factor was in fact predicted with the highest probability to associate with the TEEGR-silenced genes (Fig. 5d), consistent with the NF-κB targeting of the vast majority of these genes already identified using ChIP-seq analyses[15–17]. NF-κB is a family of dimeric transcription factors consisting of homo- or heterodimers of different subunits[18]. Although TEEGR neither altered the subunit mRNA expression (Supplementary Fig. 7d) nor the nuclear translocation of either RelA (p65; Supplementary Fig. 7e) or c-Rel following *T. gondii* infection, it selectively repressed the transcriptional activity of the dimer (Fig. 5e). The TEEGR property to selectively inhibit TNF-α-induced transcription of several NF-κB-dependent genes led us to test whether TEEGR could counteract NF-κB activation in response to exogenous TNF-α. Although tachyzoites carrying type II allele of GRA15 and TNF-α were shown separately to increase *IL-6* and *CCL20* mRNA levels, a cumulative effect was observed when tachyzoite-infected cells were stimulated with TNF-α (Supplementary Fig. 6d). Importantly, *IL-6* and *CCL20* levels were

enhanced by *teegr*-deficient parasites, thus highlighting the TEEGR ability to interfere with cell responsiveness to exogenous TNF-α (Supplementary Fig. 6d). However, TEEGR-mediated repression did not completely shut down the activation of NF-κB by GRA15-II, as WT parasites still enhance TNF-α-induced transcription despite having TEEGR (Supplementary Fig. 6d).

We next investigated whether the TEEGR-dependent EZH2-associated gene repression could act by thwarting the NF-κB response induced by *T. gondii*. We first identified 71 TEEGR-repressed genes that were previously described as silenced by EZH2 (indicated in blue in Fig. 5b and Supplementary Table 1)[19–21]. These included *IL-6* and *IL-8*, both of which re-gained activity in the presence of GSK126, a highly selective inhibitor of EZH2-methyltransferase activity (Supplementary Fig. 7f)[22]. We applied ChIP scanning to determine whether, following infection, EZH2 was recruited to cytokine genes, such as *IL-6* and *IL-8*, that are co-regulated by EZH2 and RelA/RelB in breast cancer cells[20]. In cells infected with WT TEEGR-expressing tachyzoites (type II), EZH2 was found to be markedly enriched on the *IL-6* and *IL-8* promoters concomitant to a high level of H3K27me3 (Fig. 5f). This was no longer true for cells infected by *teegr*-deficient type II tachyzoites (Fig. 5f), which instead produced increased quantities of *IL-6* and *IL-8* mRNA (Fig. 5c and Supplementary Fig. 6). These data provide evidence that, by promoting EZH2 recruitment to NF-κB target genes, TEEGR acts upstream of NF-κB and drives gene downregulation, thereby counterbalancing the typical early induction of TNF-α signalling by the *T. gondii* type II strain.

***Teegr* deficiency associates with the control of parasite burden in mice.** To explore how TEEGR could counterbalance the type II-specific activation of NF-κB in vivo, we monitored parasite multiplication and dissemination as well as BALB/c mice survival following intraperitoneal delivery of WT or *teegr*-deficient tachyzoites. Although all mice inoculated with either 10^5 or 10^6 WT tachyzoites succumbed within 6–17 d post inoculation, those infected with the same doses of *teegr*-deficient strains survived (Fig. 6a and Supplementary Fig. 8a). The mice inoculated with tachyzoites from the PruΔ*ku80*Δ*teegr* complemented with a TEEGR-HF-tagged version showed a significant but incomplete gain in virulence (Fig. 6a). The partial phenotype rescue could be caused by a decrease in activity and/or lower expression level of the chimeric version of TEEGR compared with the endogenous one. Non-invasive bioluminescence imaging highlighted a substantial gap in WT and Δ*teegr* parasite population sizes as early as day 5 post inoculation, which further increased with time (Fig. 6b and Supplementary Fig. 8b). The WT parasites continued proliferating until the mice died (that is, at day 8 post inoculation), whereas the *teegr*-deficient population expanded in the first week post inoculation, albeit to a lesser extent than the WT one, and then retracted to a few foci, compatible with both host survival (Fig. 6b and Supplementary Fig. 8b) and parasite persistence. However, when delivered per os with a low dose of cyst-containing bradyzoites, the mice that were chronically infected with *teegr*-deficient parasites had a lower number of cysts in their brain compared with the parental strain (Supplementary Fig. 8c), which therefore suggests a positive contribution of TEEGR to *T. gondii* persistence.

Given the drastic retraction of the *teegr*-deficient *T. gondii* population, we then assessed whether Δ*teegr* deficiency could make intracellular tachyzoites more susceptible to immune killing. A major defence mechanism of innate immunity against *T. gondii* is mediated by the IFN-γ–inducible IRG pathway[23]. Interestingly, unlike unstimulated human (Supplementary Fig. 8e) or mouse BMDMs (Supplementary Fig. 8d), *teegr*-deficiency correlated with increased parasite clearance in murine BMDMs pre-stimulated with a low dose of IFNγ before *T. gondii* infection (Supplementary Fig. 8d). Although our data do not support a role for Irgb6 coating of the parasitophorous vacuole membrane in the clearance of Δ*teegr* tachyzoites in stimulated macrophages (Supplementary Fig. 8f), they suggest that parasite killing could be due to either IRG evasion[24] or the recruitment of other IRG family members at the parasitophorous vacuole membrane. Overall, they certainly provide some explanation for the strong *teegr*-deficient *T. gondii* phenotype observed in vivo.

To better explain the in vivo loss of virulence shown by *teegr*-deficient *T. gondii*, we monitored the early recruitment of myeloid cells in the peritoneal cavity of mice inoculated with either TEEGR WT or *teegr*-deficient type II tachyzoites. The homing of neutrophils ($CD11b^+Gr1^{high}Ly6G^+$) and activated inflammatory monocytes ($CD11b^+Gr1^{int}Ly6G^-$), the latter of which play a critical role downstream of IL-12–IFN-γ induction to control the first amplification wave of tachyzoites in mice[25,26], was kept similar in mice inoculated with a high dose of *teegr*-deficient tachyzoites, yet those mice showed reduced myeloid cell infiltration (Supplementary Fig. 9a). This suggests that the restriction of the *teegr*-deficient population was not driven by an increase in $Gr1^+$ monocyte recruitment.

Lethal infections with type II strains are usually associated with massive overstimulation of T-helper 1 (T_H1) cell-associated cytokines, which contribute to tissue destruction[27]. Whereas extremely high serum levels of inflammatory cytokines (for example IL-12, IFN-γ and IL-18) were induced during lethal infections caused by a high dose of the WT strain, Δ*teegr* infections were typified by a low level of the T_H1-polarizing cytokine IL-12 and less circulating IL-18 and IFN-γ at day 7 post inoculation, probably as a consequence of parasite-load control (Fig. 6c and Supplementary Fig. 9b). Intriguingly, IL-1β had a peculiar pattern of secretion in vivo throughout acute infection. When a high dose of PruΔ*ku80* was inoculated, IL-1β levels declined at day 4 post inoculation after an initial rise, whereas inoculation with Δ*teegr* tachyzoites caused a sustained induction of the cytokine even when the parasite burden became barely detectable, indicating that TEEGR is also able to repress *IL-1β* expression in vivo, at least in the early stages of infection (Fig. 6c). In vitro, IL-1β levels were also slightly higher in the medium of BMDMs infected by Δ*teegr* tachyzoites. In the case of oral infection with Δ*teegr* cysts, the tissue damage was reduced (Supplementary Fig. 10a,b), while the parasite burden stayed low (Supplementary Fig. 10c) and associated with a similar cytokine signature typified by a lower level of IFN-γ and an increased level of *IL-1β* in the ileum (Supplementary Fig. 10d). These data are consistent with those reporting a protective role for IL-1 against lethal *T. gondii* infection in vivo[28,29], yet more data are needed to support a direct role of IL-1β in the control of Δ*teegr*-parasite burden.

Discussion

The highly polarized T_H1-type host response to a cystogenic *T. gondii* strain—typified by IL-12 secretion and IFN-γ induction—accounts for the restriction of the tachyzoite population through IFN-γ signalling. Meanwhile, the *T. gondii* counter-defences offset these IFN-γ-regulated innate immune defences, allowing colonization and persistence in deep tissues. The TgIST effector recently reported to co-opt host chromatin repressors and dampen STAT1-dependent IFN-γ signalling[6,7] provides proof of concept. Our present findings reveal another path taken by *T. gondii* to block the T_H1 response, which relies on the effector TEEGR. TEEGR teams up with the E2F–DP transcription factors to promote EZH2 activation, which eventually antagonizes the positive regulation of NF-κB activity by tachyzoites.

The diversity of the NF-κB family members, which in mammals include five proteins, that form numerous homo- and heterodimers, provides high selectivity in the NF-κB-mediated transcriptional response. Remarkably, *T. gondii* can differentially modulate the NF-κB pathway, depending on the parasite genotype and the host cell lineage. Thus, GRA15 from the type-II background contributes

to a sustained NF-κB p65 activation and hence to the release of pro-inflammatory cytokines such as IL-12[30] and IL-1β[31]. In addition, type II strains elicit c-Rel nuclear translocation in a Myr1-dependent but GRA15-independent manner, thereby suggesting that another GRA effector could account for the activation of c-Rel. As mice deficient in *c-Rel* are highly susceptible to the acute phase of *T. gondii* intraperitoneal infection, this pathway certainly contributes towards mounting resistance to the tachyzoite expansion[32].

Importantly, because unchecked cytokine activation has dire consequences on tissue integrity, the maintenance of immune homeostasis requires a negative feedback system. Negative regulatory mechanisms of NF-κB include, among others, the de novo synthesis of IκB-α, which shuts off the signal[18]. With TEEGR, we have discovered a negative regulator in the NF-κB signalling system that by restraining the inflammatory response sets the proper conditions for parasite persistence. Intriguingly, TEEGR selectively repressed the transcription of a subset of NF-κB-regulated cytokines (IL-1β, IL-6, IL-23A and IL-15) and chemokines (IL-8 and CCL20) without altering the expression of other NF-κB-regulated cytokines (IL-12 and IL-18; see model in Fig. 6d). A possible explanation is that TEEGR counteracts the combined activities of both GRA15[30] and still-unidentified factors that direct NF-κB nuclear translocation without impacting the sustained p38α phosphorylation mediated by GRA24 that similarly shifts the macrophage polarization toward a M1 phenotype[5]. Alternatively, this would fit with the recurrent observation that the chromatin state at different promoter classes dictates the kinetics of the NF-κB response. In this respect, lineage-defining transcription factors prime the chromatin and thereby govern the NF-κB-controlled transcriptional programs[33]. In line with this model, the TEEGR-induced EZH2 may contribute to generate a silenced chromatin landscape that would restrict NF-κB accessibility in a cell-specific manner. Interestingly, it was recently reported that although tachyzoites induce IL-1β in primary human monocytes, they inhibit IL-1β production in human neutrophils from the same blood donors by impairing the activation of the NF-κB signalling pathway[34]. Whether TEEGR plays a role in this human neutrophil-restricted phenotype merits investigation.

In conclusion, TEEGR can be seen as an 'epigenator signal'[35] in the host cell that timeously triggers the EZH2-mediated epigenetic phenotype but not subsequent events. Whether TEEGR is able to sustain a 'transcriptional memory' in tachyzoite-loaded cells (macrophage, dendritic and T cells) over the immunological tachyzoite clearance is yet to be determined. Clearly, TEEGR contributes to the diversity of GRA effectors that may reflect the large number of different hosts infected by *T. gondii*. In this respect, *T. gondii* has evolved a distinct set of effectors that target central hubs of immune signalling pathways and act synergically or antagonistically to govern the fate of *T. gondii* parasitism[8].

Methods

Mouse and experimental infection. BALB/cJRj mice were obtained from Charles River Laboratories. Mouse care and experimental procedures were performed under pathogen-free conditions in accordance with established institutional guidance (European Directive 2010/63/ EU) and approved protocols from the institutional Animal Care (PHTA) and Use Committee of University Grenoble Alpes (agreement no. C3851610006/APAFIS no. 4536-2016031017075121). BALB/cJRj female mice between six and eight weeks of age were used in all experiments. The mice were challenged by intraperitoneal injection of *T. gondii* tachyzoites or per os with cysts. The per cent cumulative mortality was defined as the number of animals that succumbed to infection/the total number of infected animals (that is, number of deaths plus seropositive survivors). We used randomization to reduce bias in mice selection and outcome assessment. Blinding was used during data collection by assigning numbers to the mice in the studies in place of genotype and infection status. We have carefully chosen the sample size based on empirical evidence of what is necessary for interpretation of the data and statistical significance. For statistical analyses of the mice survival data, the log-rank (or Mantel–Haenszel) and the Peto and Peto modification of the Gehan–Wilcoxon test were used.

Parasites and host cells. Human primary fibroblast (ATCC, CCL-171), human primary astrocytes (Science Cell Laboratories, cat no. 1800), T-REx-293 (RRID:CVCL_D585), L929 (Sigma-Aldrich, cat. no. 85011425), J774 (J774A.1; Sigma-Aldrich, cat. no. 91051511), RAW264.7 (RRID:CVCL_0493, ATCC, cat. no. TIB-71) and THP1-Blue NF-κB (InvivoGen, cat. no. thp-nfkb) cell lines were cultured in DMEM medium (Invitrogen) supplemented with 10% heat-inactivated fetal bovine serum (FBS; Invitrogen), 10 mM HEPES buffer pH 7.2, 2 mM L-glutamine and 50 μg ml^{-1} penicillin and streptomycin (Invitrogen). Human astrocytes (ScienCell Research Laboratories) were cultured in Astrocyte medium (ScienCell Research Laboratories). Cells were incubated at 37 °C in 5% CO_2. The *T. gondii* strains used in this study are listed in Supplementary Table 1. All *T. gondii* strains were maintained in vitro by serial passage on monolayers of HFFs. The strains used in this study were PruΔ*ku80*, RHΔ*ku80* and 76K–GFP–LUC (a gift from M. Grigg, National Institutes of Health). The cultures were free of mycoplasma, as determined by qualitative PCR.

Generation of BMDMs. BMDMs were obtained from female C57BL/6 mice. Bone marrow was isolated by flushing hind tibias and femurs using a 25-gauge needle followed by passages through an 18-gauge needle to disperse cell clamps. Cells were suspended in DMEM supplemented with 10% heat-inactivated FBS and 20 ng ml^{-1} recombinant M-CSF (Invitrogen), and incubated in a tissue-culture-treated flask for 8–12 h. Non-adherent cells were then harvested and transferred to 55 cm^2 non-tissue-culture-treated plates (Corning) at 4–6 × 10^6 cells plate^{-1} and further incubated at 37 °C with 5% CO_2 in humidified air. After 6 d, the cells were washed with PBS to remove non-adherent cells, harvested by dislodging with a cell scraper in ice-cold PBS and replated for the assay. This method yielded a highly pure population of F4/80+ macrophages by IFA.

Reagents. Primary antibodies mouse to HA (Roche, RRID:AB_2314622), MIC2 (provided by D. Sibley, Washington University School of Medicine), toxofilin (provided by I. Tardieux, IAB), GRA7, E2F3 (Sigma-Aldrich, RRID:AB_1841394), E2F4 (Sigma-Aldrich, RRID:AB_1841395), E2F3 (Santa Cruz Biotechnology, RRID:AB_2096807), E2F4 (Santa Cruz Biotechnology, RRID:AB_2097106 and AB_2097104), TFDP-1 (Sigma-Aldrich, RRID:AB_259233), EZH2 (Cell Signaling Technology, RRID:AB_10694683 and AB_10694383), EZH2 (BD, RRID:AB_2102429), H3K27me3 (Diagenode, RRID:AB_2616049) and TBP1 (Abcam, RRID:AB_306337) were used in the immunofluorescence, immunoblotting and/or ChIP assays. Immunofluorescence secondary antibodies were coupled with either Alexa Fluor 488 or Alexa Fluor 594 (Thermo Fisher Scientific). The secondary antibodies used in western blotting were conjugated to alkaline phosphatase (Promega) or horseradish peroxidase.

Immunofluorescence microscopy. *T. gondii*-infected HFF cells grown on coverslips were fixed in 3% formaldehyde for 20 min at room temperature, permeabilized with 0.1% (v/v) Triton X-100 for 15 min and blocked in PBS containing 3% (w/v) BSA. The cells were then incubated for 1 h with primary antibodies, followed by the addition of secondary antibodies conjugated to either Alexa Fluor 488 or 594 (Molecular Probes). The nuclei were stained for 10 min at room temperature with Hoechst 33258. The coverslips were mounted on a glass slide with Mowiol mounting medium, images were acquired with a fluorescence ZEISS ApoTome.2 microscope and processed using ZEN software (Zeiss).

Western blotting. Proteins were separated by SDS–PAGE, transferred to a polyvinylidene fluoride membrane (Immobilon-P, EMD Millipore) by liquid transfer and the western blots were probed using the appropriate primary antibodies followed by alkaline phosphatase- or horseradish peroxidase-conjugated goat secondary antibodies. The signals were detected using NBT–BCIP (Amresco) substrate solution or an enhanced chemiluminescence system (Thermo Scientific).

***T. gondii* transfection.** Vectors were transfected into RHΔ*ku80*, PruΔ*ku80* or 76K–GFP-LUC tachyzoites by electroporation. Electroporation was conducted in a 2-mm cuvette in a BTX ECM 630 (Harvard Apparatus) at 1,100 V, 25 Ω and 25 μF. Stable integrants were selected in media containing 1 μM pyrimethamine and cloned by limiting dilution.

293-T-REx transfection. The cells were plated in six-well tissue-culture dishes 24 h before transfection. HA–FLAG-fusion protein-expressing plasmids (3 mg) and 0.3 mg puromycin selection plasmid were co-transfected into 293-T-REx cells with lipofectamine 2000 reagent (Invitrogen) according to the manufacturer's instructions. The cells were diluted in the presence of 5 mg ml^{-1} puromycin (Sigma-Aldrich) for selection 72 h later. Individual drug-resistant clones were expanded and tested for tetracycline-inducible gene expression.

Quantitative real-time PCR. Cells were either uninfected or infected with the PruΔ*ku80*, PruΔ*ku80*Δ*teegr* and PruΔ*ku80*Δ*teegr* TEEGR+ strains (m.o.i. = 6) for 18 h and subsequently subjected or not to TNFα stimulation (50 ng ml^{-1}; Sigma-Aldrich) for 6 h. Total RNA was isolated using TRIzol reagent (Thermo Fisher Scientific). Complementary DNA was synthetized with random hexamers using the High Capacity RNA-to-cDNA kit (Applied Biosystem). Samples were analysed

by real-time quantitative PCR for *iNOS*, *Alox12*, *Kiss1R*, *IL-1β*, *IL-6*, *IL-8*, *IL-23A* and *CCL20* using the TaqMan gene expression master mix (Applied Biosystem) according to the manufacturer's instructions. The internal control gene *β2-microglobulin* was used for normalization. The statistical significance of differences between data means was evaluated using an unpaired, two-tailed Student's *t*-test and by non-parametric analysis of variance with multiple-comparisons.

Quantification of *T. gondii* cysts in the brains of mice. Ten weeks post infection, a half brain of each of the recipient mice was homogenized in 1 ml PBS. The numbers of cysts in ten aliquots (20 µl each) of the homogenized brain-tissue suspensions were counted microscopically.

Bioluminescence imaging. Non-invasive bioluminescence imaging was performed at 0, 2, 5, 7 and 10 d after *T. gondii* infection (5×10^4 tachyzoites). Five minutes before imaging, vigil mice received an intraperitoneal injection of 150 µg g^{-1} D-luciferin (Promega), and were then anaesthetized (isoflurane 4% for induction and 1,5% thereafter) and placed in an optical imaging system (IVIS Kinetic, PerkinElmer). This allowed localization of luciferase-positive *T. gondii* and evaluation of the abdominal load. Bioluminescence signal was expressed as the number of photons per second.

Flow cytometry. Six-week-old BALB/cJRj mice (Charles River) were intraperitoneally infected with 5×10^5 parasites and killed on days 2, 4 and 7 post inoculation. Immediately after being killed, the mice were peritoneally lavaged with PBS and the recovered lavage fluid was centrifuged at 500*g* for 8 min. Peritoneal cells were washed once with PBS. Harvested cells were suspended in stain buffer (PBS containing 2% FBS and 0.1 mM EDTA), seeded in 96-well plates (10^6 cells per 100 µl) and pretreated with FcBlock (clone 2.4G2; BD Biosciences) for 30 min at 4 °C. The cells were then incubated with the following antibodies fluorescently conjugated to cell surface markers (BD Biosciences): PE-conjugated anti-CD11b, PE-conjugated anti-Gr1 (clone RB6-8C5), PE-conjugated anti-F4/80 and APC-conjugated anti-Ly6G. Isotype controls consisted of PE-conjugated rat IgG2b, PE-conjugated rat IgG2a and APC-conjugated rat IgG2a (BD Biosciences). The analysis of stained cells was performed with a FACSCalibur flow cytometer (BD Biosciences). For all samples, 100,000 cells were analysed for plot generation.

Harvest of peritoneal contents, in vivo cytokine ELISA and determination of the parasite load. Six-week-old BALB/cJRj mice (Charles River) were intraperitoneally infected with 10^5 parasites and killed on days 2, 4, 7 and 9 post inoculation. Immediately after being killed, the mice were peritoneally lavaged with 3 ml physiological serum. Of the recovered lavage fluid, 2 ml was centrifuged at 20,000*g* for 15 min at 4 °C and the clarified supernatant was stored at −70 °C until analysis by ELISA. The protein concentrations of IFN-γ, IL-18, IL-1β, TNFα, IL-12, IL-23 and IL-22 were determined using commercially available ELISA kits (IL-18 ELISA kit, MBL International; IL-1β Quantikine ELISA kit, R&D Systems; IFN-γ ELISA kit, BD Biosciences and TNFα, IL-12, IL-23 and IL-22 ELISA kits, Thermo Fisher Scientific) according to the manufacturer's instructions. The parasite loads in the peritoneal content were quantified after DNA extraction (QIAamp DNA mini kit, QIAGEN) using the quantitative PCR targeting of the *T. gondii*–specific 529-bp repeat element.

Histological analysis of ileum. Fragments of the small intestines of mice infected with WT or *teegr*-deficient cysts were harvested on day 8 post-infection, fixed in 10% buffered formalin and paraffin processed. Tissue sections that were 5 µm thick were mounted on slides and stained with haematoxylin and eosin. The histological score was analysed with the following parameters: intensity of the lamina propria inflammatory infiltration, thickening of lamina propria, destruction of the villi and necrosis, which were evaluated by intensity, represented as arbitrary units ranging from zero (less intense or absent) to six (highly intense) for each parameter. The final histological score is a sum of each parameter for each mouse.

Microarray hybridization and data analysis. Human (primary fibroblasts and astrocytes) and murine (BMDM) cells were either uninfected or infected with the Pru*Δku80*, Pru*Δku80*ΔTEEGR and Pru*Δku80Δteegr* TEEGR strains (m.o.i. = 6) for 18 h. Total RNA was extracted and purified using TRIzol (Invitrogen). The RNA quantity and quality were measured using a NanoDrop 2000 (Thermo Scientific). Transcripts were obtained from three biological replicates each. RNA labelling and array hybridization were performed by Array Star Inc. Briefly, RNA quantity and quality were first measured by a NanoDrop ND-1000. The RNA integrity was assessed by standard denaturing agarose gel electrophoresis. Transcripts were obtained from three biological replicates for each sample. Total RNA from each sample was linearly amplified and labelled with Cy3-UTP. The labelled antisense RNAs (cRNAs) were purified using an RNeasy mini kit (Qiagen). The concentration and specific activity of the labelled cRNAs (pmol Cy3 per µg of cRNA) were measured by a NanoDrop ND-1000. The labelled cRNA (1 µg each) was fragmented by adding 11 µl 10×Blocking Agent and 2.2 µl 25×Fragmentation Buffer, then heated at 60 °C for 30 min and finally 55 µl 2×GE Hybridization Buffer was added to dilute the labelled cRNA. Hybridization solution (100 µl) was dispensed into the gasket slide and assembled to the gene-expression microarray slide. The slides were incubated for 17 h at 65 °C in an Agilent hybridization oven. Agilent Feature Extraction software (version 11.0.1.1) was used to analyse the acquired array images. Quantile normalization and subsequent data processing were performed using the GeneSpring GX v12.1 software (Agilent Technologies). After quantile normalization of the raw data, genes that in at least 3 of 27 samples had flags in Detected ('All Targets Value') were chosen for further data analysis. Differentially expressed genes with statistical significance were identified through volcano plot filtering. Hierarchical clustering was performed using the R software (version 2.15). Gene Ontology (GO) and pathway analyses were performed in the standard enrichment computation method. The thresholds were fold change ≥2.0 and $P \leq 0.05$. GO and Kyoto Encyclopedia of Genes and Genomes pathway analyses were performed using the DAVID bioinformatics resources. Microarray data has been uploaded to GEO datasets under the accession numbers GSE113618 and GSE113626. GSEA (http://software.broadinstitute.org/gsea/index.jsp) was used to find candidate transcription factors and canonical pathways that are modulated differently between *T. gondii* infections. This program uses a priori defined sets of genes and determines whether the members of these sets of genes are randomly distributed throughout a ranked list or primarily found at the top or bottom. As GSEA is generally used to generate hypotheses, gene sets enriched with a FDR <0.25 were considered significant. Both transcription-factor and canonical-pathway gene sets from the Molecular Signatures Database were evaluated for enrichment. DiRE of co-regulated genes (https://dire.dcode.org/) was also used. For every gene in a list, DiRE detects regulatory elements throughout the entire gene locus and looks for enrichment of TFBSs.

Plasmid constructs. The plasmids and primers used in this work are listed in Supplementary Table 1. To construct vectors pLIC-TEEGR-HF, the coding sequence of *TEEGR* was amplified using the primers LIC-239010-F and LIC-239010-R and genomic DNA of RH*Δku80* or Pru*Δku80* strains of *T. gondii* as the DNA templates. The resulting PCR product was cloned into the above pLIC vectors using the ligation independent cloning (LIC) method. The truncated versions of *TEEGR* were cloned as described above in the pLIC-HF-*dhfr* vector. The forward primer LIC-TEEGR-F was used with reverse primers LIC-TEEGR-QPV-REV or LIC-TEEGR-TNR-REV to construct the vectors pLIC-TEEGR-ΔSER–HA–FLAG and pLIC-TEEGR-ΔR3–HA–FLAG, respectively. We constructed pcDNA-TEEGR-HA–FLAG by amplifying the TEEGR coding sequence from residue 29 to 744 with primers TEEGR-pcDNA4-Cter-FWD and TEEGR-pcDNA4-Cter-REV. The resulting PCR products were cloned into the pcDNA-LIC–HA–FLAG plasmid using the LIC method. The engineered LIC cassette of this vector fuses the C-terminal end of the protein of interest with an AGAGAGA linker followed by an HA–FLAG tag. The vectors pDEST14 KO *TEEGR*^{I} and pDEST14 KO *TEEGR*^{II} were generated to construct the deletion/insertion mutation of *TEEGR* in *T. gondii* strains RH*Δku80* (type I) and Pru*Δku80* (type II), respectively. The MultiSite Gateway Pro Three-Fragment Recombination system was used to clone the *dhfr* cassette flanked by the 5′ and 3′ surrounding regions of the *TEEGR* coding sequence of type I and type II genomic DNA. The *dhfr* cassette, which confers resistance to pyrimethamine, was amplified by PCR using primers attB4r-5′dhfr F and attB3r-3′dhfr R and the plasmid pDHFR-TSc3 as the DNA template. The resulting PCR product was cloned in pDONR221 P4r-P3r according to the manufacturer's instructions, yielding the vector pDONR221/DHFR. The 5′ flanking region of *TEEGR* was amplified using the primers attB1-TEEGR_F and attB4-TEEGR_R, and was cloned into the plasmid pDONR221 P1-P4. The 3′ flanking region of *TEEGR* was amplified using the primers attB3-TEEGR_F and attB2-TEEGR_R, and was cloned into the plasmid pDONR221 P3-P2. The resulting vectors, pDONR221/5′*TEEGR* and pDONR221/3′*TEEGR*, respectively, were then recombined with the pDONR221/DHFR into the destination vector pDEST14, yielding the pDEST14 KO *TEEGR*. TEEGR^{Nter}-R3-HA–FLAG was DNA synthesised and cloned in pLIC-DHFR. To generate a complemented Pru*Δku80Δteegr* strain, the vector pLIC-P_{TEEGR}-*TEEGR*–HA–FLAG was co-electroporated with the pMiniHX at a 1:10 ratio followed by selection with mycophenolic acid and xanthine, and cloned by limiting dilution. The resulting strain is named Pru*Δku80Δteegr*, pLIC-P_{TEEGR}-*TEEGR*–HA–FLAG (Supplementary Table 3). The plasmid pTOXO_Cas9-CRISPR::sgTEEGR vector was generated as previously described[6]. Briefly, the primers TEEGR-CRISP-FWD and TEEGR-CRISP-REV containing the sgRNA targeting the TEEGR genomic sequence were phosphorylated, annealed and ligated in the pTOXO_Cas9–CRISPR plasmid linearized with BsaI, yielding pTOXO_Cas9–CRISPR–GFP_sgTEEGR.

Chromatographic purification of TEEGR-containing complex. Nuclear extracts from 293-T-REx cells stably expressing HA–FLAG-tagged protein or J774 cells infected with Pru*Δku80* or RH*Δku80* expressing HA–FLAG-tagged TEEGR, were incubated with anti-FLAG M2 affinity gel (Sigma-Aldrich) for 1 h at 4 °C. Beads were washed with ten column volumes of BC500 buffer (20 mM Tris–HCl, pH 8.0, 500 mM KCl, 20% glycerol, 1 mM EDTA, 1 mM dithiothreitol, 0.5% NP-40 and protease inhibitors). The bound polypeptides were eluted stepwise with 250 µg ml^{-1} FLAG peptide (Sigma-Aldrich) diluted in BC100 buffer. For size-exclusion chromatography, protein eluates were loaded onto a Superose 6 HR 10/30 column equilibrated with BC500. The flow rate was fixed at 0.35 ml min^{-1} and 0.5-ml fractions were collected.

Mass spectrometry-based proteomics. Protein bands were excised from colloidal blue-stained gels (Thermo Fisher Scientific), treated with dithiothreitol and iodoacetamide to alkylate the cysteines before in-gel digestion using modified trypsin (Promega; sequencing grade). The resulting peptides from individual bands were analysed by online nano liquid chromatography tandem mass spectrometry (UltiMate 3000 coupled to LTQ-Orbitrap Velos, Thermo Scientific) using a 25-min gradient. Peptides and proteins were identified using Mascot (Matrix Science) and filtered using IRMa software: only rank 1 peptides exhibiting a query identity threshold above 0.02 and a score superior to 20 were selected before protein grouping.

ChIP assay. HFF cells were either uninfected or infected for 24 h with PruΔ*ku80* TEEGR–HA–FLAG or PruΔ*ku80* Δ*teegr*. Cells were then cross-linked with 1% formaldehyde for 10 min before quenching with 125 mM glycine for 5 min. The ChIP assay was performed by using the Transcription Factor Chromatin Immunoprecipitation kit (Diagenode) according to the manufacturer's protocol. In brief, fixed cells were sonicated to shear the cross-linked chromatin into an average DNA fragment size of 200–600 bp. We used 40×10^6 sorted nuclei in 300 µl immunoprecipitation buffer supplemented with fresh proteinase inhibitors. By using a Diagenode Bioruptor precooled to 4 °C, shearing was achieved in 1.5-ml-low-binding tubes in the appropriate tube adaptor with 18 high-energy cycles of 30 s on and 30 s off. The aforementioned antibodies were used for immunoprecipitation. After an overnight incubation, the DNA–protein–antibody complex was eluted. The crosslinks were reversed by heating the samples at 65 °C for 4 h. DNA was purified by using IPure kit (Diagenode) according to the manufacturer's protocol. For validation, quantitative real-time ChIP-PCR was performed by SYBR Green (Applied Biosystems) using StepOnePLus (Applied Biosystems). Real-time PCR was performed and then quantitated using the delta–delta CT (ΔΔCT) method. The primer sequences are listed in Supplementary Table 3.

NF-κB reporter assay. THP1-Blue NF-κB cells (InvivoGen) were grown in RPMI 1640 medium supplemented with 10% (v/v) FBS, 2 mM L-glutamine, 100 U ml^{-1} penicillin, 100 µg ml^{-1} streptomycin, 25 mM HEPES, 100 µg ml^{-1} Normocin and 10 µg ml^{-1} blasticidin. THP1-Blue NF-κB cells were treated with TNFα or infected with WT or Δ*teegr* PruΔ*ku80* strains and then followed by determination of NF-κB activity using a reporter gene assay. QUANTI-Blue (InvivoGen) was added to the cells, the plates were incubated for a further 2 h and the optical density at 630 nm was recorded. The graphs show the results from averaged technical replicates and at least three independent experiments.

Reporting Summary. Further information on research design is available in the Nature Research Reporting Summary linked to this article.

Data availability

Correspondence and requests for materials should be addressed to M.-A.H. The microarray data have been deposited to the GEO datasets under the accession numbers GSE113618 and GSE113626.

Received: 8 May 2018; Accepted: 18 March 2019;
Published online: 29 April 2019

References

1. Jeffers, V., Tampaki, Z., Kim, K. & Sullivan, W. J. A latent ability to persist: differentiation in *Toxoplasma gondii*. *Cell. Mol. Life Sci.* **75**, 2355–2373 (2018).
2. Melo, M. B., Jensen, K. D. C. & Saeij, J. P. J. *Toxoplasma gondii* effectors are master regulators of the inflammatory response. *Trends Parasitol.* **27**, 487–495 (2011).
3. Hunter, C. A. & Sibley, L. D. Modulation of innate immunity by *Toxoplasma gondii* virulence effectors. *Nat. Rev. Microbiol.* **10**, 766–778 (2012).
4. Bougdour, A. et al. Host cell subversion by *Toxoplasma* GRA16, an exported dense granule protein that targets the host cell nucleus and alters gene expression. *Cell Host Microbe* **13**, 489–500 (2013).
5. Braun, L. et al. A *Toxoplasma* dense granule protein, GRA24, modulates the early immune response to infection by promoting a direct and sustained host p38 MAPK activation. *J. Exp. Med.* **210**, 2071–2086 (2013).
6. Gay, G. et al. *Toxoplasma gondii* TgIST co-opts host chromatin repressors dampening STAT1-dependent gene regulation and IFN-γ-mediated host defenses. *J. Exp. Med.* **213**, 1779–1798 (2016).
7. Olias, P., Etheridge, R. D., Zhang, Y., Holtzman, M. J. & Sibley, L. D. *Toxoplasma* effector recruits the Mi-2/NuRD complex to repress STAT1 transcription and block IFN-γ-dependent gene expression. *Cell Host Microbe* **20**, 72–82 (2016).
8. Hakimi, M.-A., Olias, P. & Sibley, L. D. *Toxoplasma* effectors targeting host signaling and transcription. *Clin. Microbiol. Rev.* **30**, 615–645 (2017).
9. Fischer, M., Grossmann, P., Padi, M. & DeCaprio, J. A. Integration of TP53, DREAM, MMB-FOXM1 and RB-E2F target gene analyses identifies cell cycle gene regulatory networks. *Nucleic Acids Res.* **44**, 6070–6086 (2016).
10. Marson, A. et al. Foxp3 occupancy and regulation of key target genes during T-cell stimulation. *Nature* **445**, 931–935 (2007).
11. Julian, L. M. et al. Tissue-specific targeting of cell fate regulatory genes by E2f factors. *Cell Death Differ.* **23**, 565–575 (2016).
12. Zheng, N., Fraenkel, E., Pabo, C. O. & Pavletich, N. P. Structural basis of DNA recognition by the heterodimeric cell cycle transcription factor E2F–DP. *Gene Dev.* **13**, 666–764 (1999).
13. Margueron, R. & Reinberg, D. The Polycomb complex PRC2 and its mark in life. *Nature* **469**, 343–349 (2011).
14. Bracken, A. P. et al. EZH2 is downstream of the pRB-E2F pathway, essential for proliferation and amplied in cancer. *EMBO J.* **22**, 5323–5335 (2003).
15. Garber, M. et al. A high-throughput chromatin immunoprecipitation approach reveals principles of dynamic gene regulation in mammals. *Mol. Cell* **47**, 810–822 (2012).
16. Xing, Y., Zhou, F. & Wang, J. Subset of genes targeted by transcription factor NF-κB in TNFα-stimulated human HeLa cells. *Funct. Integr. Genomics* **13**, 143–154 (2013).
17. Luo, X., Chae, M., Krishnakumar, R., Danko, C. G. & Kraus, W. Dynamic reorganization of the AC16 cardiomyocyte transcriptome in response to TNFα signaling revealed by integrated genomic analyses. *BMC Genom.* **15**, 155 (2014).
18. Afonina, I. S., Zhong, Z., Karin, M. & Beyaert, R. Limiting inflammation—the negative regulation of NF-κB and the NLRP3 inflammasome. *Nat. Immunol.* **18**, 861–869 (2017).
19. Sun, F. et al. Combinatorial pharmacologic approaches target EZH2-mediated gene repression in breast cancer cells. *Mol. Cancer Ther.* **8**, 3191–3202 (2009).
20. Lee, S. T. et al. Context-specific regulation of NF-κB target gene expression by EZH2 in breast cancers. *Mol. Cell* **43**, 798–810 (2011).
21. Liu, Y. et al. Epithelial EZH2 serves as an epigenetic determinant in experimental colitis by inhibiting TNFα-mediated inflammation and apoptosis. *Proc. Natl Acad. Sci. USA* **114**, E3796–E3805 (2017).
22. McCabe, M. T. et al. EZH2 inhibition as a therapeutic strategy for lymphoma with EZH2-activating mutations. *Nature* **492**, 108–112 (2012).
23. Howard, J. C., Hunn, J. P. & Steinfeldt, T. The IRG protein-based resistance mechanism in mice and its relation to virulence in *Toxoplasma gondii*. *Curr. Opin. Microbiol.* **14**, 414–421 (2011).
24. Virreira Winter, S. et al. Determinants of GBP recruitment to *Toxoplasma gondii* vacuoles and the parasitic factors that control it. *PLoS ONE* **6**, e24434 (2011).
25. Robben, P. M., LaRegina, M., Kuziel, W. A. & Sibley, L. D. Recruitment of Gr-1$^+$ monocytes is essential for control of acute toxoplasmosis. *J. Exp. Med.* **201**, 1761–1769 (2005).
26. Dunay, I. R. et al. Gr1(+) inflammatory monocytes are required for mucosal resistance to the pathogen *Toxoplasma gondii*. *Immunity* **29**, 306–317 (2008).
27. Mordue, D. G., Monroy, F., La Regina, M., Dinarello, C. A. & Sibley, L. D. Acute toxoplasmosis leads to lethal overproduction of Th1 cytokines. *J. Immunol.* **167**, 4574–4584 (2001).
28. Chang, H. R., Grau, G. E. & Pechère, J. C. Role of TNF and IL-1 in infections with Toxoplasma gondii. *Immunology* **69**, 33–37 (1990).
29. Hunter, C. A., Chizzonite, R. & Remington, J. S. IL-1 beta is required for IL-12 to induce production of IFN-gamma by NK cells. A role for IL-1 beta in the T cell-independent mechanism of resistance against intracellular pathogens. *J. Immunol.* **155**, 4347–4354 (1995).
30. Rosowski, E. E. et al. Strain-specific activation of the NF-κB pathway by GRA15, a novel *Toxoplasma gondii* dense granule protein. *J. Exp. Med.* **208**, 195–212 (2011).
31. Gorfu, G. et al. Dual role for inflammasome sensors NLRP1 and NLRP3 in murine resistance to *Toxoplasma gondii*. *mBio* **5**, e01117-13 (2014).
32. Mason, N. J., Liou, H.-C. & Hunter, C. A. T cell-intrinsic expression of c-Rel regulates Th1 cell responses essential for resistance to *Toxoplasma gondii*. *J. Immunol.* **172**, 3704–3711 (2004).
33. Bhatt, D. & Ghosh, S. Regulation of the NF-κB-mediated transcription of inflammatory genes. *Front. Immunol.* **5**, 71 (2014).
34. Lima, T. S., Gov, L. & Lodoen, M. B. Evasion of human neutrophil-mediated host defense during *Toxoplasma gondii* infection. *mBio* **9**, e02027-17 (2018).
35. Berger, S. L., Kouzarides, T., Shiekhattar, R. & Shilatifard, A. An operational definition of epigenetics. *Genes Dev.* **23**, 781–783 (2009).
36. Lee, B. K., Bhinge, A. A. & Iyer, V. R. Wide-ranging functions of E2F4 in transcriptional activation and repression revealed by genome-wide analysis. *Nucleic Acids Res.* **39**, 3558–3573 (2011).

Acknowledgements

This work was supported by the Laboratoire d'Excellence (LabEx) ParaFrap (ANR-11-LABX-0024), the Agence Nationale pour la Recherche (Project HostQuest, ANR-18-CE15-0023) and the European Research Council (ERC Consolidator grant no. 614880 Hosting TOXO to M.-A.H.). The proteomic experiments were partly supported by the Agence Nationale pour la Recherche (Investissement d'Avenir Infrastructures, ProFi project ANR-10-INBS-08-01).

Author contributions

M.-A.H., L.B. and A.B. conceived the project. L.B., M.-P.B.-P., P.-M.H., D.C., S.K.-J., J.V., V.J., B.T., Y.C., I.T. and A.B. designed, performed and interpreted the experimental work. M.-A.H. supervised the research. M.-A.H. wrote the paper with editorial support from I.T., L.B. and A.B.

Competing interests

The authors declare no competing interests.

Additional information

Supplementary information is available for this paper at https://doi.org/10.1038/s41564-019-0431-8.

Correspondence and requests for materials should be addressed to A.B. or M.-A.H.

nature research

Corresponding author(s): Mohamed-ali HAKIMI / Alexandre BOUGDOUR
NMICROBIOL-18050844

Reporting Summary

Nature Research wishes to improve the reproducibility of the work that we publish. This form provides structure for consistency and transparency in reporting. For further information on Nature Research policies, see Authors & Referees and the Editorial Policy Checklist.

Statistical parameters

When statistical analyses are reported, confirm that the following items are present in the relevant location (e.g. figure legend, table legend, main text, or Methods section).

n/a	Confirmed	
☐	☒	The exact sample size (*n*) for each experimental group/condition, given as a discrete number and unit of measurement
☐	☒	An indication of whether measurements were taken from distinct samples or whether the same sample was measured repeatedly
☐	☒	The statistical test(s) used AND whether they are one- or two-sided *Only common tests should be described solely by name; describe more complex techniques in the Methods section.*
☐	☒	A description of all covariates tested
☒	☐	A description of any assumptions or corrections, such as tests of normality and adjustment for multiple comparisons
☐	☒	A full description of the statistics including central tendency (e.g. means) or other basic estimates (e.g. regression coefficient) AND variation (e.g. standard deviation) or associated estimates of uncertainty (e.g. confidence intervals)
☐	☒	For null hypothesis testing, the test statistic (e.g. *F*, *t*, *r*) with confidence intervals, effect sizes, degrees of freedom and *P* value noted *Give P values as exact values whenever suitable.*
☒	☐	For Bayesian analysis, information on the choice of priors and Markov chain Monte Carlo settings
☐	☒	For hierarchical and complex designs, identification of the appropriate level for tests and full reporting of outcomes
☐	☒	Estimates of effect sizes (e.g. Cohen's *d*, Pearson's *r*), indicating how they were calculated
☐	☒	Clearly defined error bars *State explicitly what error bars represent (e.g. SD, SE, CI)*

Our web collection on statistics for biologists may be useful.

Software and code

Policy information about availability of computer code

Data collection	Agilent Feature Extraction software (version 11.0.1.1) was used to analyze the acquired array images. Quantile normalization and subsequent data processing were performed with using the GeneSpring GX v12.1 software (Agilent Technologies). After quantile normalization of the raw data, genes that at least 3 out of 27 samples have flags in Detected ("All Targets Value") were chosen for further data analysis.
Data analysis	Hierarchical Clustering was performed using the R software (version 2.15). KEGG (Kyoto Encyclopedia of Genes and Genomes) pathway analysis were performed using the DAVID Bioinformatics Resources. Gene set enrichment analysis (GSEA, http://software.broadinstitute.org/gsea/index.jsp) was used to find candidate transcription factors and canonical pathways. Distant Regulatory Elements of co-regulated genes (DiRE, https://dire.dcode.org/) was also used.

For manuscripts utilizing custom algorithms or software that are central to the research but not yet described in published literature, software must be made available to editors/reviewers upon request. We strongly encourage code deposition in a community repository (e.g. GitHub). See the Nature Research guidelines for submitting code & software for further information.

Data

Policy information about availability of data

All manuscripts must include a data availability statement. This statement should provide the following information, where applicable:

- Accession codes, unique identifiers, or web links for publicly available datasets
- A list of figures that have associated raw data
- A description of any restrictions on data availability

Microarray data has been uploaded to GEO Datasets under accession number (GSE113618).

Field-specific reporting

Please select the best fit for your research. If you are not sure, read the appropriate sections before making your selection.

☒ Life sciences ☐ Behavioural & social sciences ☐ Ecological, evolutionary & environmental sciences

For a reference copy of the document with all sections, see nature.com/authors/policies/ReportingSummary-flat.pdf

Life sciences study design

All studies must disclose on these points even when the disclosure is negative.

Sample size	Sample size estimation was not performed.
Data exclusions	no data exclusions
Replication	All the experiments were performed at least in triplicate independent experiments in accordance with well-established reporting procedures for all the assays.
Randomization	We used randomization to reduces bias in mice selection and outcome assessment.
Blinding	Blinding was used during data collection by assigning numbers in place of genotype and infection status to mice in the studies.

Reporting for specific materials, systems and methods

Materials & experimental systems

n/a	Involved in the study
☒	☐ Unique biological materials
☐	☒ Antibodies
☐	☒ Eukaryotic cell lines
☒	☐ Palaeontology
☐	☒ Animals and other organisms
☒	☐ Human research participants

Methods

n/a	Involved in the study
☒	☐ ChIP-seq
☒	☐ Flow cytometry
☒	☐ MRI-based neuroimaging

Antibodies

Antibodies used	Primary antibodies mouse anti-HA (Roche, RRID:AB_2314622), MIC2 (provided by D. Sibley, Washington University School of Medicine, St Louis, MO), Toxofilin (provided by I. Tardieux, IAB, Grenoble, France), GRA7, E2F3 (Sigma-Aldrich, RRID:AB_1841394), E2F4 (Sigma-Aldrich, RRID:AB_1841395), E2F3 (Santa Cruz Biotechnology, RRID:AB_2096807), E2F4 (Santa Cruz Biotechnology, RRID:AB_2097106 and AB_2097104), TFDP-1 (Sigma-Aldrich, RRID:AB_259233), EZH2 (Cell Signaling Technology, RRID:AB_10694683 and AB_10694383), EZH2 (BD, RRID:AB_2102429), H3K27me3 (Diagenode, RRID:AB_2616049) and TBP1 (Abcam, RRID:AB_306337)
Validation	Validation data ara available at manufacters website.

Eukaryotic cell lines

Policy information about cell lines

Cell line source(s)	Human primary fibroblasts (ATCC® CCL-171™), Human primary Astrocytes (Science Cell Laboratories, cat #1800), T-Rex-293 cell line (RRID:CVCL_D585), L929 cell line (Sigma-Aldrich Cat# 85011425), J774 cell line (J774A.1, Sigma-Aldrich Cat# 91051511), RAW264.7 cell line (ATCC Cat# TIB-71, RRID:CVCL_0493) and THP1-Blue™ NF-κB Cells cell line (InvivoGen Cat # thp-nfkb)
Authentication	none of them were authenticated
Mycoplasma contamination	The cultures were free of mycoplasma, as determined by qualitative PCR.
Commonly misidentified lines (See ICLAC register)	*Name any commonly misidentified cell lines used in the study and provide a rationale for their use.*

Animals and other organisms

Policy information about studies involving animals; ARRIVE guidelines recommended for reporting animal research

Laboratory animals	BALB/cJRj and BL6 mice were obtained from Charles River Laboratories.
Wild animals	This study did not involve wild animals.
Field-collected samples	This study did not involve samples collected from the field.